A Journal of the Gesellschaft Deutscher Chemiker

Angewandte International Edition Chemie

GDCh

www.angewandte.org

Accepted Article

Title: A Fluorescent Probe for Rapid, High-Contrast Visualization of Folate-Receptor-Expressing Tumors in Vivo

Authors: Koji Numasawa, Kenjiro Hanaoka, Naoko Saito, Yoshifumi Yamaguchi, Takayuki Ikeno, Honami Echizen, Masahiro Yasunaga, Toru Komatsu, Tasuku Ueno, Masayuki Miura, Tetsuo Nagano, and Yasuteru Urano

To be cited as: *Angew. Chem. Int. Ed.* 10.1002/anie.201914826
Angew. Chem. 10.1002/ange.201914826

Link to VoR: http://dx.doi.org/10.1002/anie.201914826
http://dx.doi.org/10.1002/ange.201914826

WILEY-VCH

10.1002/anie.201914826

WILEY-VCH

RESEARCH ARTICLE

A Fluorescent Probe for Rapid, High-Contrast Visualization of Folate-Receptor-Expressing Tumors *in Vivo*

Koji Numasawa,[a] *Kenjiro Hanaoka,**[a] *Naoko Saito,*[a] *Yoshifumi Yamaguchi,*[a,b] *Takayuki Ikeno,*[a] *Honami Echizen,*[a] *Masahiro Yasunaga,*[c] *Toru Komatsu,*[a] *Tasuku Ueno,*[a] *Masayuki Miura,*[a] *Tetsuo Nagano,*[d] *and Yasuteru Urano**[a,e,f]

Abstract: *Folate receptors (FRs) are membrane proteins involved in folic acid uptake, and the alpha isoform (FR-α) is overexpressed in ovarian and endometrial cancer cells. For fluorescence imaging of FRs in vivo, the near-infrared (NIR) region (650–900 nm), where tissue penetration is high and autofluorescence is low, is optimal, but existing NIR fluorescent probes targeting FR-α show high non-specific tissue adsorption, and require prolonged washout to visualize tumors. We have designed and synthesized a new NIR fluorescent probe,* ***FolateSiR-1****, utilizing a Si-rhodamine fluorophore having a carboxy group at the benzene moiety, coupled to a folate ligand moiety via a negatively charged tripeptide linker. This probe exhibits very low background fluorescence, and afforded a tumor-to-background ratio (TBR) of up to 83 in FR-expressing tumor-bearing mice within 30 min. Thus,* ***FolateSiR-1*** *has the potential to contribute to the research in the field of biology and the clinical medicine.*

Introduction

Folic acid, which is required in one-carbon metabolic reactions and for the synthesis of nucleotide bases, emerged as a targeting ligand for imaging of cancer tissues in the 1990s.[1,2] It is internalized into cells via folate receptors (FRs) expressed on the cell surface. The alpha isoform of folate receptor (FR-α) is upregulated in about 40% of human cancers, especially in malignant tissues such as ovarian cancer, whereas normal tissues, except for the kidney, do not accumulate folic acid or its conjugates.[3-5] Folic acid binds to FR-α with high affinity (K_d about 10^{-9} M) even after conjugation to imaging agents, and undergoes receptor-mediated endocytosis.[3] Consequently, various folate-linked drugs and imaging agents have been developed.[1-3] Among available imaging modalities, fluorescence imaging provides real-time images with millimeter resolution, and has attracted interest for intraoperative fluorescence imaging of tumor tissues.[6] For example, 90-95% of epithelial ovarian cancers overexpress FR-α, and a folate-linked fluorescent dye, folate-FITC, was recently employed for intraoperative tumor-specific fluorescence imaging in patients.[7] However, FITC emits green fluorescence (around 520 nm), and is unsuitable for imaging deep tissues. For this purpose, dyes emitting in the near-infrared (NIR) region (650–900 nm) are most useful, because tissue penetration is high and autofluorescence is low, resulting in a low background signal.[8,9] However, existing folate-linked NIR fluorescent dyes show nonspecific adsorption on tissues, and require a washout period of up to 24 h to clearly image tumors in tumor-bearing mice (Scheme 1).[10-12] Therefore, we aimed to develop a NIR fluorescent probe suitable for rapid, high-contrast detection of FR-expressing tumors *in vivo*, without the need for a washout procedure.

Two approaches have so far been used to improve the signal-to-background ratio (SBR) of fluorescent probes. One approach is to develop activatable fluorescent probes whose fluorescence signal is emitted only in response to a specific feature of the local environment, such as pH. For example, a probe targeting human epidermal growth factor receptor type 2 (HER2) employed a fluorescent dye-labeled antibody that is fluorescently activated in the low pH environment of lysosomes after cellular internalization.[13] This approach provides a high tumor-to-normal-tissue signal ratio. However, endocytotic transport of the probe to lysosomes takes up to 24 h. Yang *et al.* designed and synthesized an off/on-type fluorescent probe for detection of FRs by utilizing a pH-sensitive acyl hydrazone linker and a dark quencher, but failed to observe fluorescence enhancement after cellular internalization.[14] They also developed a folate conjugate whose fluorescence wavelength is changed by reduction of disulfide in the probe structure during receptor-mediated endocytosis.[15] The latter probe was suitable for cellular applications, but the half-time of disulfide reduction was as long as 6 h after endocytosis. The second approach is to minimize nonspecific adsorption of the probe *in vivo*. Choi *et al.* reported that the zwitterionic heptamethine indocyanine NIR fluorophore ZW800-1 exhibits low

[a] Dr. K. Numasawa, Prof. K. Hanaoka, N. Saito, Prof. Y. Yamaguchi, T. Ikeno, H. Echizen, Dr. T. Komatsu, Dr. T. Ueno, Prof. M. Miura, Prof. Y. Urano
Graduate School of Pharmaceutical Sciences, The University of Tokyo
7-3-1 Hongo, Bunkyo-ku, Tokyo 113-0033 (Japan)
E-mail: uranokun@mol.f.u-tokyo.ac.jp (Y.U.), khanaoka@mol.f.u-tokyo.ac.jp (K.H.)
[b] Prof. Y. Yamaguchi
Institute of Low Temperature Science, Hokkaido University
Sapporo 060-0819 (Japan)
[c] Dr. M. Yasunaga
Division of Developmental Therapeutics, Research Center for Innovative Oncology, National Cancer Center Hospital East
6-5-1 Kashiwanoha, Kashiwa, Chiba 277-8577 (Japan)
[d] Prof. T. Nagano
Drug Discovery Initiative, The University of Tokyo
7-3-1 Hongo, Bunkyo-ku, Tokyo 113-0033 (Japan)
[e] Prof. Y. Urano
Graduate School of Medicine, The University of Tokyo
7-3-1 Hongo, Bunkyo-ku, Tokyo 113-0033 (Japan)
[f] Prof. Y. Urano
CREST (Japan) Agency for Medical Research and Development (AMED)
1-7-1 Otemachi, Chiyoda-ku, Tokyo 100-0004 (Japan)

Supporting information for this article is given via a link at the end of the document.

10.1002/anie.201914826
WILEY-VCH

RESEARCH ARTICLE

serum-protein binding, ultralow nonspecific tissue background and rapid elimination from the body through renal filtration.[16] In tumor model applications, a tumor-to-background ratio (defined as the contrast-to-background ratio in the tumor divided by the contrast-to-background ratio in nearby normal tissue) of over 17 was achieved at 4 h after injection of ZW800-1 conjugated to cRGD. Here, we build on this approach to design and synthesize an NIR fluorescent probe that we believe offers sufficiently high performance for practical *in vivo* imaging.

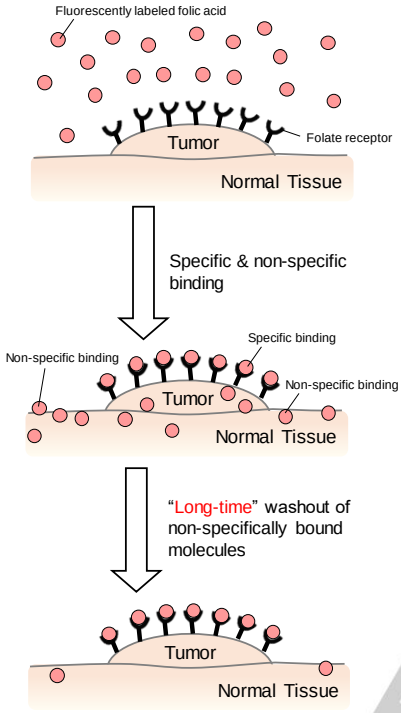

Scheme 1. Imaging strategy of existing near-infrared fluorescent probes for *in vivo* fluorescence imaging of whole animals.

Results and Discussion

First, we needed a system to assess the occurrence of nonspecific adsorption of folate-linked NIR fluorescent dyes. For this purpose, we performed live-cell fluorescence imaging of FR-α-expressing and FR-α-non-expressing cultured cells, i.e., KB cells (FR+) and OVCAR-3 cells (FR–), with a commercially available NIR fluorescent probe, **FolateRSense 680** (PerkinElmer, USA). The expression of FRs on these cells was confirmed by immunostaining (Figure S1). KB cells showed strong fluorescence at the cell membrane due to probe binding to FR-α on the cell surface, but we also observed some bright dots inside the cells, apparently due to nonspecific internalization of the probe (Figure S2a). On the other hand, OVCAR-3 cells showed many very bright dots within the cells (Figure S2b). Therefore, we considered that this cellular imaging system was suitable to judge whether or not our newly synthesized folate-linked fluorescent dyes might show nonspecific adsorption when used for *in vivo* fluorescence imaging.

In the molecular design of our folate-linked fluorescent dyes, we chose to conjugate the linker moiety to the folate glutamate moiety (Figure 1a). The crystal structure of human FR-α complexed with folic acid has the folate pteroate moiety buried inside FR, whereas the glutamate moiety is exposed to the solvent and protrudes from the binding pocket entrance, so that it can be conjugated with a fluorescent dye without adversely affecting the binding to FR-α.[17] By this molecular design, we expected that fluorescent probes would show the high affinity for FR, i.e., K_d around 10^{-9} M, because folate conjugates (and folic acid) normally bind to FR with this affinity.[3] We also employed a negatively charged peptide linker, Asp-Lys-Gly, in order to reduce the cell-membrane permeability of the folate-linked fluorescent dye, and we attached various xanthene fluorophores to the amino group of the lysine side chain in the linker (Figure 1a and Figure S3). We applied each compound to the live-cell fluorescence imaging with KB cells and OVCAR-3 cells. As shown in Figure S3, basically fluorescein derivative-labeled folates such as **Fluorescein Folate**, **2-Me DCTM Folate** and **2-COOH DCTM Folate** showed the selective detection of FR in living cells, while rhodamine derivatives-labeled folate such as **TAMRA Folate** and **Alexa488 Folate** stained the cell membrane of KB cells, but they also showed nonspecific adsorption. Among them, we fortunately found a promising NIR fluorescent probe for detecting FR, **FolateSiR-1**, along with a control compound, **FolateSiR-2**, which has very similar chemical structure to **FolateSiR-1** (Figure 1a). Both **FolateSiR-1** and **FolateSiR-2** showed similar absorption and emission spectra in the NIR region, and their fluorescence quantum yields were 7.6% and 5.1%, respectively (Figure 1). The

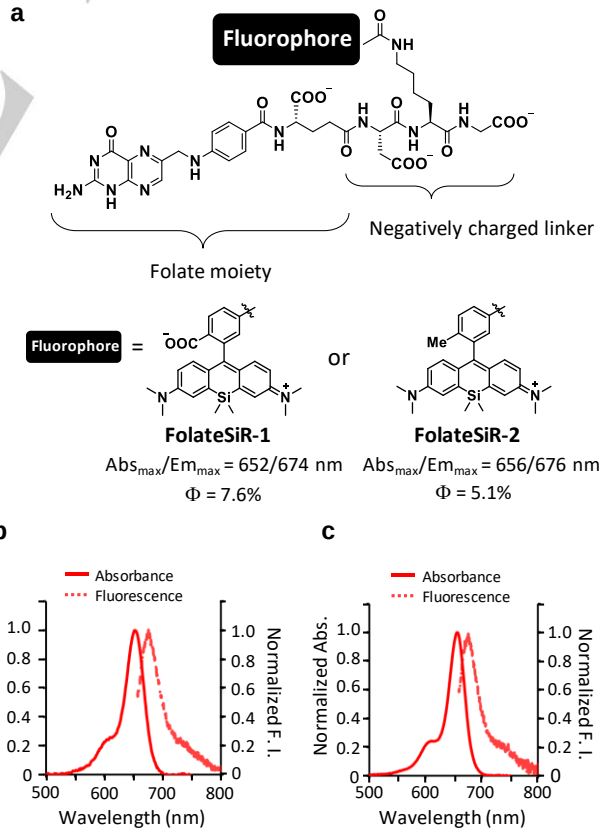

10.1002/anie.201914826

Figure 1. a) Molecular design of fluorescent probes for detection of folate receptors. The structures of **FolateSiR-1** and **FolateSiR-2** are also shown. **b)** Absorption and emission spectra of 1 μM **FolateSiR-1** in 100 mM sodium phosphate buffer at pH 7.4. Excitation wavelength: 652 nm. **c)** Absorption and emission spectra of 1 μM **FolateSiR-2** in 100 mM sodium phosphate buffer at pH 7.4. Excitation wavelength: 656 nm.

relatively low fluorescence quantum yields were probably due to dynamic quenching between the fluorophore and the electron-rich pteroate moiety,[18] but are sufficiently high for cellular and *in vivo* fluorescence imaging. When we applied **FolateSiR-1** to KB cells, the cell membrane was clearly stained; there were no bright dots inside the cells, and the fluorescence disappeared in the presence of 1 mM folic acid as a competitor (Figure 2a), indicating that nonspecific endocytosis of **FolateSiR-1** did not occur. **FolateSiR-1** may also possess the low cell-membrane permeability owing to the relatively large molecular weight and the negatively charged peptide linker. Further, when we applied **FolateSiR-1** to OVCAR-3 cells, almost no fluorescence was observed, supporting the idea that there is little nonspecific adsorption of the dye (Figure 2b). On the other hand, **FolateSiR-2** stained the cell membrane of KB cells, but also exhibited many bright dots inside the cells both in the presence and absence of 1 mM folic acid (Figure 2a). It also afforded some bright dots inside OVCAR-3 cells, supporting the existence of nonspecific adsorption (Figure 2b). Although folate receptors can normally induce cell uptake of ligands via endocytosis, the endocytosis of **FolateSiR-1** and **FolateSiR-2** via folate receptors was not observed. In short, **FolateSiR-1** showed a high S/N ratio with little nonspecific adsorption in cellular fluorescence imaging.

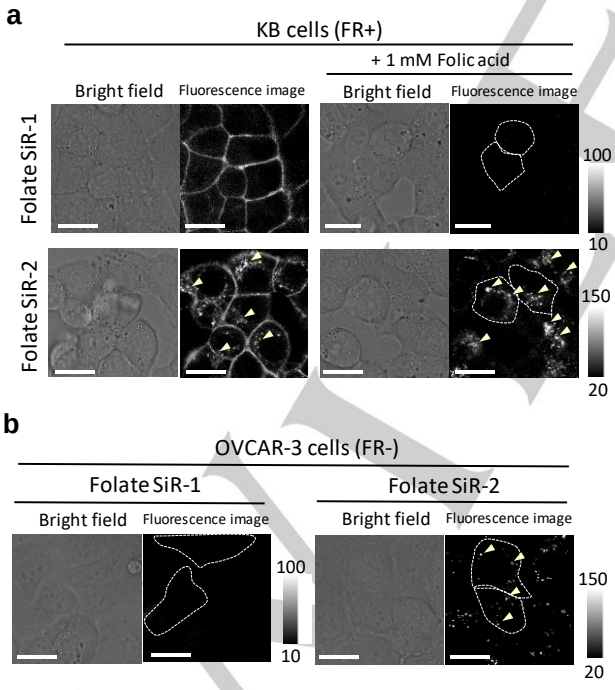

Figure 2. a) Bright-field (left) and fluorescence (right) images of KB cells incubated with 5 μM **FolateSiR-1** or **FolateSiR-2** in the presence or absence of 1 mM folic acid and 0.5% DMSO as a cosolvent. White arrows indicate bright dots inside cells. Ex. 650 nm, Em. 670-750 nm. Scale bars: 20.0 μm. **b)** Bright-field (left) and fluorescence (right) images of OVCAR-3 cells incubated with 5 μM **FolateSiR-1** or **FolateSiR-2** and 0.5% DMSO as a cosolvent. White arrows indicate bright dots inside cells. Ex. 650 nm, Em. 670-750 nm. Scale bars: 20 μm.

Next, we applied these two fluorescent probes to *ex vivo* mouse embryos to visualize endogenously expressed folate-binding protein 1 (Folbp1), the mouse analogue of human FR-α. Periconceptional folate supplementation significantly reduces the risk of neural tube defects, and Folbp1 is one of the membrane proteins that mediate cellular uptake of folate; mice lacking Folbp1 are defective in early embryonic development.[19] Maternal anti-FR antibodies are also associated with neuronal tube defects in humans.[20] *In situ* hybridization revealed a distinct expression pattern of *Folbp1* mRNA in the neural folds prior to the initiation of neural tube closure at the cervical region and the prosencephalic/mesencephalic boundary.[21] *Folbp1* mRNA is mainly localized to the most dorsal regions of the neural folds, where fusion takes place, and as neural fold fusion proceeds, *Folbp1* mRNA expression extends to the adjacent unfused neural folds (Figure 3a). However, the expression pattern of Folbp1 protein has not been reported.

We firstly applied **FolateSiR-1** to embryos at day 8.5 postcoitum. The living embryos were stained with 20 μM **FolateSiR-1** for 30 min at 37˚C and fluorescence imaging was quickly performed. The neural tube closing region showed strong fluorescence compared with other regions, while weak fluorescence was observed throughout the embryo (Figure 3b). On the other hand, we observed strong, speckled fluorescence throughout the whole embryo when **FolateSiR-2** was loaded (Figure 3c), suggesting the idea that **FolateSiR-2** binds non-specifically in the cells. We then performed a competition experiment of **FolateSiR-1** with 1 mM folic acid. The fluorescence images changed with time, probably because embryogenesis is rapid, so in this experiment we fixed the embryos with 4% formaldehyde after staining with **FolateSiR-1**. We confirmed that **FolateSiR-1** was retained in the cell membrane of KB cells after the fixation process (Figure S4a). Fluorescence imaging of the **FolateSiR-1**-stained, fixed embryos showed a similar pattern of strong fluorescence in the neural tube closing region to that shown in Figure 3b (Figure S4b and Figure S5). This pattern disappeared in the presence of 1 mM folic acid (Figure S4c). Thus, **FolateSiR-1** appears to stain Folbp1-expressing regions in a folic acid-competitive manner.

10.1002/anie.201914826

WILEY-VCH

RESEARCH ARTICLE

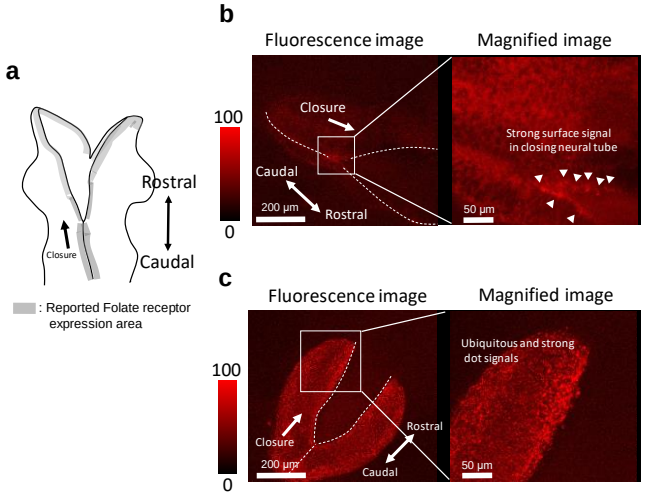

Figure 3. a) Schematic illustration of folate receptor (= Folbp 1) expression in mouse embryo; regions reported to show folate receptor expression are shown in gray. b) Fluorescence image of mouse embryo incubated with 20 μM **FolateSiR-1**. Locations stained with **FolateSiR-1** are indicated by white arrowheads. c) Fluorescence image of mouse embryo incubated with 20 μM **FolateSiR-2**.

We further applied **FolateSiR-1** to *in vivo* fluorescence imaging of tumors in mouse models. **FolateSiR-1** was intravenously injected via the tail vein into tumor-bearing mice prepared by subcutaneous inoculation of KB cells. FR-α-expressing tumors were clearly visualized with an extremely low background (TBR up to 83) just 30 minutes after injection of **FolateSiR-1** (Figure 4a,b). The mice were sacrificed, and we confirmed that **FolateSiR-1** was strongly accumulated in the tumor (fluorescence in the stomach may have been derived from the feed in this experiment) (Figure S6a). On the other hand, relatively strong fluorescence throughout the whole body was observed at the same time-point after injection of **FolateSiR-2**, resulting in a low TBR (Figure 4c). Even at 6 h after injection of **FolateSiR-2**, the fluorescence was relatively strong throughout the whole body and the TBR was around 12, which was much lower than that of **FolateSiR-1** (Figure 4c,d), though tumor accumulation of **FolateSiR-2** was observed in excised tissues (Figure S6b). We also prepared an FR(-)-tumor model by subcutaneous injection of HT1080 cells. The absence of FR was confirmed by immunostaining (Figure S1). No fluorescence was observed when **FolateSiR-1** was injected into these mice (Figure S7). On the other hand, when we injected **FolateSiR-2** into these mice, fluorescence rapidly appeared throughout the whole body (Figure S8); it subsequently decreased with time, but the tumor was not visualized. Moreover, when we injected 6 mM folic acid in saline into KB tumor-bearing mouse, followed by 100 μM **FolateSiR-1** in saline (100 μL), no fluorescence was observed except in the intestine, which might be due to the feed (Figure S9). These results indicate that **FolateSiR-1** binds specifically to FR-expressing tumors in these mice, affording high-contrast images unlike typical NIR fluorescent probes such as **FolateSiR-2**.

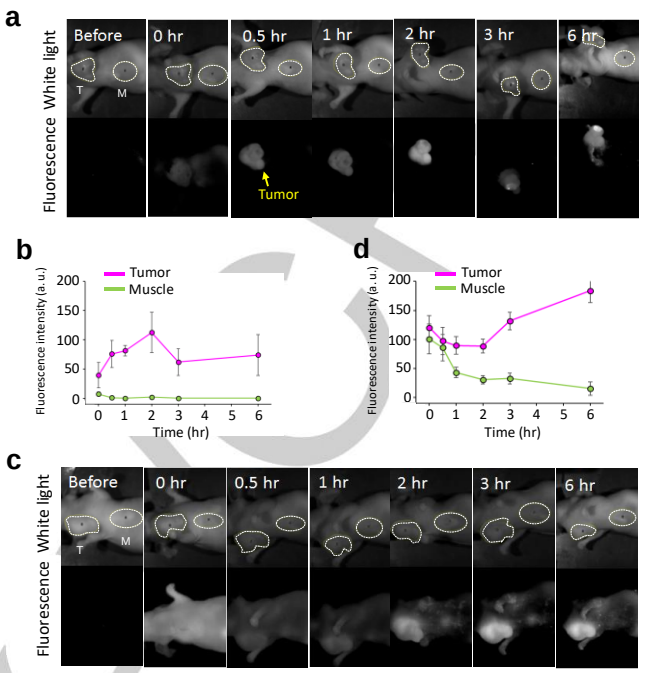

Figure 4. a) Time-lapse fluorescence images of KB tumor-bearing mouse injected with 100 μM **FolateSiR-1** in 100 μL saline containing 1% DMSO as a cosolvent. Fluorescence and white light images were obtained before and 0, 0.5, 1, 2, 3 and 6 h after the probe injection. Ex. 661 (641-681) nm, Em. 700-800 nm. T: tumor, M: muscle. Fluorescence intensity scale: gray scale 0 to 255. b) Time-dependent change of fluorescence intensity in tumor and non-tumor (muscle) areas of three mice, including the mouse in (a). Error bar shows S.E. c) Time-lapse fluorescence images of KB tumor-bearing mouse injected with 100 μM **FolateSiR-2** in 100 μL saline containing 1% DMSO as a cosolvent. Fluorescence and white-light images were obtained before and 0, 0.5, 1, 2, 3 and 6 h after the probe injection. Ex. 661 (641-681) nm, Em. 700-800 nm. T: tumor, M: muscle. Fluorescence intensity scale: gray scale 0 to 255. d) Time-dependent change of fluorescence intensity in tumor and non-tumor (muscle) areas of three mice, including the mouse in (c). Error bar shows S.E.

To further investigate the potential applicability of **FolateSiR-1** for intraoperative tumor detection, we utilized a tissue microarray of patient-derived ovarian tumor tissues and normal tissues from regions adjacent to tumors (Figure S10). **FolateSiR-1** successfully visualized ovarian tumor tissues, while exhibiting little binding to normal tissues (Figure 5a and Figure S11). Furthermore, the fluorescence image of the tissue microarray closely matched the immunostaining image (Figure 5b, Figure S12 and Figure S13), confirming the ability of **FolateSiR-1** to visualize human tumors *ex vivo*. The selective staining of tumor tissues by **FolateSiR-1** was also observed in a specimen of tissue microarray, which contains both tumor tissues and non-tumor tissues (vascular tissues and fibrous tissues) (Figure S13c).

10.1002/anie.201914826

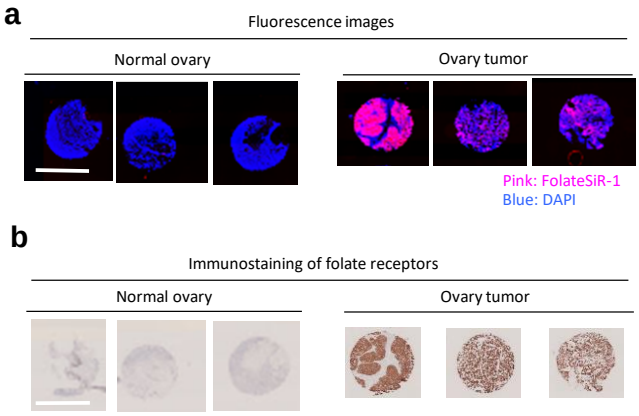

Figure 5. a) The ovarian cancer tissue microarray was incubated with 5 μM **FolateSiR-1** and 2.9 μM DAPI (nuclear stain) in phosphate-buffered saline containing 0.05% Tween 20 (PBST) for 2 h. Then, the tissue microarray was washed with PBST three times and the fluorescence image was obtained. The microarray contains 37 tumor tissues and 3 normal tissues. Fluorescence images of the 3 normal tissues and 3 representative tumor tissues are shown. The scale bar represents 2 mm. b) Immunostaining of folate receptors in the tissue microarray. The immunostained 3 normal tissues and 3 tumor tissues correspond to those in (a). The scale bar represents 2 mm.

Conclusion

In this study, we designed and synthesized a series of folate-fluorescent dye conjugates. We focused on the nonspecific adsorption of typical NIR fluorescent dye such as cyanine dyes and folate conjugates to tissues inside the body when they are injected via tail vein. We conjugated various xanthene-based fluorescent dyes to folic acid and applied them to the live-cell fluorescence imaging for selection of fluorescent probes showing low nonspecific adsorption. Among xanthene fluorescent dye-conjugated folates, we fortunately found that **FolateSiR-1**, consisting of a Si-rhodamine fluorophore having a carboxy group at the benzene moiety, coupled to a folate ligand moiety via a negatively charged tripeptide linker (Figure 1a), achieved a very low level of nonspecific tissue binding. Indeed, this probe could rapidly provide high-contrast images of tumors in a mouse model *in vivo* without any washout procedure, due to the very low background fluorescence. We think the low background may be due to the combination of the intrinsic low level of nonspecific binding derived from the probe design and the preference of the 2-COOH SiR650 fluorophore for the intramolecularly spirocyclized, nonfluorescent form in hydrophobic environments, such as those in plasma/inner membranes.[22] The spirocyclization converts the cationic xanthene moiety to neutral form, whereas in contrast, the cationic charge of cyanines and Si-rhodamines favors nonspecific adsorption. Indeed, 2-COOH SiR650 showed a large absorbance decrease in 100 mM sodium phosphate buffer (pH 7.4) containing 10% fetal bovine serum, which contains many proteins (Figure S14). This idea is also supported by the observation that when **FolateSiR-1** was dissolved in mouse serum, the absorbance was significantly decreased, presumably due to nonspecific binding to proteins of mouse serum and the formation of the intramolecularly spirocyclized, nonfluorescent form Figure S15). This is also consistent with the finding of Weissleder *et al.* that a neutral 2-COOH SiR650 derivative could follow the intracellular localization of a therapeutic drug in live cells.[23-25] Notably, these ligand-2-COOH SiR650 conjugates show almost no fluorescence signal at non-targeted regions inside the cells, in accordance with the concept of using background-free “tame” fluorescent probes[26] to obtain clear fluorescence images in live cells. Our work extends the scope of this concept to *in vivo* fluorescence imaging of whole animals. Indeed, the effective blocking of nonspecific adsorption on non-targeted tissues enabled us to clearly visualize tumors within less than 30 minutes after probe injection. During the operation, at most 5 to 10 minutes may be allowed as an incubation time after probe injection, and **FolateSiR-1** has a potential to be used even during the operation. A similar approach might be applied to other tumor-related membrane proteins, such as carbonic anhydrase IX, which is overexpressed in hypoxic tumor tissues.[27]

Moreover, the NIR probe OTL-38, which is based on the cyanine fluorophore, is currently in phase II clinical trial for intraoperative imaging of ovarian cancer.[28-30] Our new probe **FolateSiR-1** might be superior to OTL-38 in terms of high S/N ratio, and we believe it should be suitable for precise intraoperative fluorescence detection of tiny tumors in the millimeter size range, as well as for the efficient endoscopic detection of cancer cells in abdominal dropsy immediately after surgical operation. Recently, therapeutic antibodies have been applied to the treatment of various types of cancer. However, although it was confirmed to be safe, anti-FRs antibody did not meet the primary endpoints of progression-free survival or overall survival in a clinical trial. Therefore, anti-FRs antibody-drug conjugates (ADCs) have been developed in order to enhance the efficacy.[31,32] However, poor penetration into solid tumors still poses a problem for ADCs as well as naked therapeutic antibodies. On the other hand, small-molecular drug conjugates are expected to overcome this issue.[33] The binding activity and specificity for FR of **FolateSiR-1** are thought to be high as well as anti-FRs antibodies,[3] and so **FolateSiR-1** might be available as a basic scaffold for the development of new small-molecular drug conjugates to treat FR-expressing ovarian cancer. Furthermore, the theranostic features of such agents could be valuable to assess the pharmacokinetic profile within the tumor tissue.

Acknowledgements

This work was supported in part by JSPS KAKENHI Grant Numbers JP18H04609 and JP16H05099 to K.H. and JP26110005 to Y.Y., SENTAN, JST to K.H, and Hoansha Foundation to K.H. This work was also supported by a grant JSPS Core-to-Core program, A. Advanced Research Networks and a Grant-in-Aid for Scientific Research on Innovative Areas “Singularity Biology (No.8007)” (JP19H05414 to K.H.) of The Ministry of Education, Culture, Sports, Science, and Technology, Japan.

Conflict of interest

The authors declare no conflict of interest.

Keywords: fluorescent probes • fluorescence • vitamins • chromophores • cancer

[1] W. Xia, P. S. Low, *J. Med. Chem.* **2010**, *53*, 6811-6824.
[2] Y. G. Assaraf, C. P. Leamon, J. A. Reddy, *Drug Resist. Update.* **2014**, *17*, 89-95.
[3] P. S. Low, S. A. Kularatne, *Curr. Opin. Chem. Biol.* **2009**, *13*, 256-262.
[4] K. R. Kalli, A. L. Oberg, G. L. Keeney, T. J. H. Christianson, P. S. Low, K. L. Knutson, L. C. Hartmann, *Gynecol. Oncol.* **2008**, *108*, 619-626.
[5] S. Markert, S. Lassmann, B. Gabriel, M. Klar, M. Werner, G. Gitsch, F. Kratz, A. Hasenburg, *Anticancer Res.* **2008**, *28*, 3567-3572.
[6] A. L. Vahrmeijer, M. Hutteman, J. R. van der Vorst, C. J. H. van de Velds, J. V. Frangioni, *Nat. Rev. Clin. Oncol.* **2013**, *10*, 507-518.
[7] G. M. van Dam, G. Themelis, L. M. A. Crane, N. J. Harlaar, R. G. Pleijhuis, W. Kelder, A. Sarantopoulos, J. S. de Jong, H. J. G. Arts, A. G. J. van der Zee, J. Bart, P. S. Low, V. Ntziachristos, *Nat. Med.* **2011**, *17*, 1315-1319.
[8] J. V. Frangioni, *Curr. Opin. Chem. Biol.* **2003**, *7*, 626-634.
[9] R. Weissleder, V. Ntziachristos, *Nat. Med.* **2003**, *9*, 123-128.
[10] W. K. Moon, Y. Lin, T. O'Loughlin, Y. Tang, D. E. Kim, R. Weissleder, C. H. Tung, *Bioconjugate Chem.* **2003**, *14*, 539-545.
[11] C. H. Tung, Y. Lin, W. K. Moon, R. Weissleder, *ChemBioChem* **2002**, *8*, 784-786.
[12] L. E. Kelderhouse, V. Chelvam, C. Wayua, S. Mahalingam, S. Poh, S. A. Kularatne, P. S. Low, *Bioconjugate Chem.* **2013**, *24*, 1075-1080.
[13] Y. Urano, D. Asanuma, Y. Hama, Y. Koyama, T. Barrett, M. Kamiya, T. Nagano, T. Watanabe, A. Hasegawa, P. L. Choyke, H. Kobayashi, *Nat. Med.* **2009**, *15*, 104-109.
[14] J. Yang, H. Chen, I. R. Vlahov, J. –X. Cheng, P. S. Low, *J. Pharmacol. Exp. Ther.* **2007**, *321*, 462-468.
[15] J. Yang, H. Chen, I. R. Vlahov, J. –X. Cheng, P. S. Low, *Proc. Natl. Acad. Sci.* **2006**, *103*, 13872-13877.
[16] H. S. Choi, S. L. Gibbs, J. H. Lee, S. H. Kim, Y. Ashitate, F. Liu, H. Hyun, G. L. Park, Y. Xie, S. Bae, M. Henary, J. V. Frangioni, *Nat. Biotechnol.* **2013**, *31*, 148-153.
[17] C. Chen, J. Ke, X. E. Zhou, W. Yi, J. S. Brunzelle, J. Li, E. –L. Yong, H. E. Xu, K. Melcher, *Nature* **2013**, *500*, 486-489.
[18] S. Gawęda, G. Stochel, K. Szaciłowski, *Chem. Asian J.* **2007**, *2*, 580-590.
[19] J. A. Piedrahita, B. Oetama, G. D. Bennett, J. van Waes, B. A. Kamen, J. Richardson, S. W. Lacey, R. G. W. Anderson, R. H. Finnell, *Nat. Genet.* **1999**, *23*, 228-232.
[20] V. Ramaekers, J. M. Sequeira, E. V. Quadros, *Clin. Chem. Lab. Med.* **2013**, *51*, 497-511.
[21] H. Saitsu, M. Ishibashi, H. Nakano, K. Shiota, *Dev. Dyn.* **2003**, *226*, 112-117.
[22] G. Lukinavičius, K. Umezawa, N. Olivier, A. Honigmann, G. Yang, T. Plass, V. Mueller, L. Reymond, I. R. Corrêa Jr., Z. –G. Luo, C. Schultz, E. A. Lemke, P. Heppenstall, C. Eggeling, S. Manley, K. Johnsson, *Nat. Chem.* **2013**, *5*, 132-139.
[23] M. A. Miller, E. Kim, M. F. Cuccarese, A. L. Plotkin, M. Prytyskach, R. H. Kohler, M. J. Pittet, R. Weissleder, *Chem. Commun.* **2018**, *54*, 42-45.
[24] E. Kim, K. S. Yang, R. H. Kohler, J. M. Dubach, H. Mikula, R. Weissleder, *Bioconjugate Chem.* **2015**, *26*, 1513-1518.
[25] E. Kim, K. S. Yang, R. J. Giedt, R. Weissleder, *Chem. Commun.* **2014**, *50*, 4504-4507.
[26] S. H. Alamudi, R. Satapathy, J. Kim, D. Su, H. Ren, R. Das, L. Hu, E. Alvarado-Martínez, J. Y. Lee, C. Hoppmann, E. Peña-Cabrera, H. –H. Ha, H. –S. Park, L. Wang, Y. –T. Chang, *Nat. Commun.* **2016**, *7*:× doi:10.1038/ncomms11964.
[27] C. T. Supuran, *Nat. Rev. Drug Discov.* **2008**, *7*, 168-181.
[28] C. E. S. Hoogstins, Q. R. J. G. Tummers, K. N. Gaarenstroom, C. D. de Kroon, J. B. M. Z. Trimbos, T. Bosse, V. T. H. B. M. Smit, J. Vuyk, C. J. H. van de Velde, A. F. Cohen, P. S. Low, J. Burggraaf, A. L. Vahrmeijer, *Clin. Cancer Res.* **2016**, *22*, 2929-2938.
[29] E. de Jesus, J. J. Keating, S. A. Kularatne, J. Jiang, R. Judy, J. Predina, S. Nie, P. Low, S. Singhal, *Int. J. Mol. Imaging* **2015**, Article ID 469047.
[30] J. –Y. Winum, *Expert Opin. Ther. Pat.* **2016**, *26*, 1223-1226.
[31] O. Ab, K. R. Whiteman, L. M. Bartle, X. Sun, R. Singh, D. Tavares, A. LaBelle, G. Payne, R. J. Lutz, J. Pinkas, V. S. Goldmacher, T. Chittenden, J. M. Lambert, *Mol. Cancer Ther.* **2015**, *14*, 1605-1613.
[32] X. Cheng, J. Li, K. Tanaka, U. Majumder, A. Z. Milinichik, A. C. Verdi, C. J. Maddage, K. A. Rybinski, S. Fernando, D. Fernando, M. Kuc, K. Furuuchi, F. Fang, T. Uenaka, L. Grasso, E. F. Albone, *Mol. Cancer Ther.* **2018**, *17*, 2665-2675.
[33] M. P. Deonarain, G. Yahioglu, I. Stamati, A. Pomowski, J. Clarke, B. M. Edwards, S. Diez-Posada, A. C. Stewart, *Antibodies* **2018**, *7*, 16.

10.1002/anie.201914826

WILEY-VCH

Entry for the Table of Contents

RESEARCH ARTICLE

The alpha isoform of folate receptor (FR-α) is overexpressed in ovarian and endometrial cancer cells. The existing NIR fluorescent probes targeting FR-α show high non-specific tissue adsorption. We have designed and synthesized a new NIR fluorescent probe, **FolateSiR-1**. This probe exhibits very low background fluorescence, and afforded a tumor-to-background ratio (TBR) of up to 83 in FR-expressing tumor-bearing mice within 30 min after the injection.

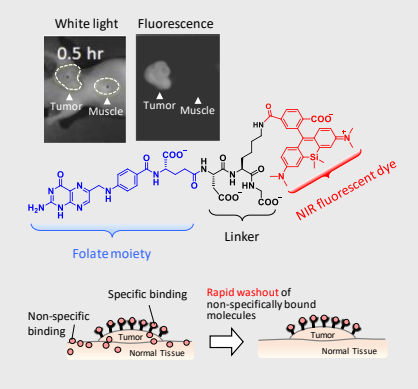

Koji Numasawa, Kenjiro Hanaoka, Naoko Saito, Yoshifumi Yamaguchi, Takayuki Ikeno, Honami Echizen, Masahiro Yasunaga, Toru Komatsu, Tasuku Ueno, Masayuki Miura, Tetsuo Nagano, Yasuteru Urano**

Page 1 – Page 6

A Fluorescent Probe for Rapid, High-Contrast Visualization of Folate-Receptor-Expressing Tumors *in Vivo*